OXFORD

Human Molecular Genetics, 2018, Vol. 27, No. 19 3313–3324

doi: 10.1093/hmg/ddy223
Advance Access Publication Date: 20 June 2018
General Article

GENERAL ARTICLE

A mutation affecting polycystin-1 mediated heterotrimeric G-protein signaling causes PKD

Stephen C. Parnell[1,2,*], Brenda S. Magenheimer[1,2], Robin L. Maser[1,2,3], Tengis S. Pavlov[4], Mallory A. Havens[5], Michelle L. Hastings[6], Stephen F. Jackson[2], Christopher J. Ward[2], Kenneth R. Peterson[1,2], Alexander Staruschenko[7] and James P. Calvet[1,2,*]

[1]Department of Biochemistry and Molecular Biology, [2]The Jared Grantham Kidney Institute, [3]Department of Clinical Laboratory Sciences, University of Kansas Medical Center, Kansas City, KS 66160, USA, [4]Division of Hypertension and Vascular Research, Henry Ford Hospital, Detroit, MI 48202, USA, [5]Department of Biology, Lewis University, Romeoville, IL 60446, USA, [6]Department of Cell Biology and Anatomy, Chicago Medical School, Rosalind Franklin University of Medicine and Science, North Chicago, IL 60064, USA and [7]Department of Physiology, Medical College of Wisconsin, Milwaukee, WI 53226, USA

*To whom correspondence should be addressed at: Department of Biochemistry and Molecular Biology and The Jared Grantham Kidney Institute, University of Kansas Medical Center, 3901 Rainbow Blvd MS3018, Kansas City, KS 66160, USA. Tel: +1 9135880705; Fax: +1 9135889251; Email: sparnell@kumc.edu (S.C.P.); Department of Biochemistry and Molecular Biology and The Jared Grantham Kidney Institute, University of Kansas Medical Center, 3901 Rainbow Blvd MS3018, Kansas City, KS 66160, USA. Tel: +1 9135887424; Fax: +1 9135889251; Email: jcalvet@kumc.edu (J.P.C.)

Abstract

Autosomal dominant polycystic kidney disease (ADPKD) is characterized by the growth of renal cysts that ultimately destroy kidney function. Mutations in the *PKD1* and *PKD2* genes cause ADPKD. Their protein products, polycystin-1 (PC1) and polycystin-2 (PC2) have been proposed to form a calcium-permeable receptor-channel complex; however the mechanisms by which they function are almost completely unknown. Most mutations in *PKD1* are truncating loss-of-function mutations or affect protein biogenesis, trafficking or stability and reveal very little about the intrinsic biochemical properties or cellular functions of PC1. An ADPKD patient mutation (L4132Δ or ΔL), resulting in a single amino acid deletion in a putative G-protein binding region of the PC1 C-terminal cytosolic tail, was found to significantly decrease PC1-stimulated, G-protein-dependent signaling in transient transfection assays. *Pkd1*$^{\Delta L/\Delta L}$ mice were embryo-lethal suggesting that ΔL is a functionally null mutation. Kidney-specific *Pkd1*$^{\Delta L/cond}$ mice were born but developed severe, postnatal cystic disease. PC1$^{\Delta L}$ protein expression levels and maturation were comparable to those of wild type PC1, and PC1$^{\Delta L}$ protein showed cell surface localization. Expression of PC1$^{\Delta L}$ and PC2 complexes in transfected CHO cells failed to support PC2 channel activity, suggesting that the role of PC1 is to activate G-protein signaling to regulate the PC1/PC2 calcium channel.

Introduction

ADPKD cyst growth leads to massive kidney enlargement and ultimately to renal failure. Mutations in the *PKD1* gene cause ~85% of ADPKD cases and those in the *PKD2* gene ~15% of ADPKD cases (1–3). *PKD1* and *PKD2* encode PC1 and PC2, respectively.

Received: January 16, 2018. **Revised:** June 5, 2018. **Accepted:** June 5, 2018

Significance Statement

ADPKD is caused by mutations in either of two genes, *PKD1* or *PKD2*, whose protein products, polycystin-1 (PC1) and polycystin-2 (PC2), are proposed to form a calcium-permeable receptor-channel complex. A single leucine deletion (ΔL) in the cytosolic C-tail of PC1 was found to cause severe ADPKD in a knock-in mouse model. Most mutations in *PKD1* affect PC1 protein levels, biogenesis, trafficking, stability or interactions with PC2 and reveal little about the biochemical function of PC1. In contrast, ΔL appears to specifically impair PC1-dependent heterotrimeric G-protein signaling and activation of the PC1/PC2 receptor-channel complex, suggesting that the function of PC1 is to regulate PC2 through heterotrimeric G-proteins.

PC1 is a large (4 303 aa) integral protein with a > 3 000 aa N-terminal extracellular domain, 11 membrane-spanning domains and a smaller C-terminal cytosolic domain of about 200 aa (4). PC1 is related to the adhesion-GPCRs and has structural features consistent with it being a membrane receptor (3,5). PC2 (TRPP2) is a member of the transient receptor potential (TRP) family of membrane channels (6). PC2 has nonspecific cation channel activity and acts as a Ca^{2+}-regulated Ca^{2+} channel (7,8). PC2 has also been shown to be an ER Ca^{2+} release channel that functions in an IP_3 receptor-dependent fashion (9). The C-tails of PC1 and PC2 directly interact via a coiled-coil interaction (10), and the complex has been shown to generate a unique Ca^{2+} signal in transfected cells (11). PC1 and PC2 are widely expressed in many embryonic and adult tissues and organs making it likely that they function together in most tissues.

Expression of the cytosolic C-tail of PC1 stimulates a number of signaling pathways in transfected cells, leading to the activation of promoter reporters such as AP-1 and NFAT (12–15). The membrane-proximal region of the PC1 C-tail contains a heterotrimeric G-protein binding and activation domain (16) that initiates signaling by activating $G_{i/o}$, $G_{q/11}$ and $G_{12/13}$ (14), and when injected into neuronal cells, PC1 has been shown to activate $G_{i/o}$ and release Gβγ subunits that modulate ion channel activity (17). Ciliary PC1 and PC2 have also been shown to mediate fluid-flow mechanosensory, transient elevations in intracellular Ca^{2+} in a ryanodine receptor-dependent fashion (18). While it appears that PC1/PC2 form a signaling-responsive Ca^{2+} channel, their ciliary mechanosensory actions and their biochemical and cellular functions are unclear (19–21).

Most mutations in *PKD1* are loss-of-function, including deletions, splicing, frameshift and nonsense mutations, which would be expected to significantly alter PC1 protein levels (22). Missense mutations have also been described that affect functional protein levels (23); however, other than revealing that PC1 biogenesis and protein levels are critical, these mutations do not provide insight into the biochemical functions of PC1. There are a number of C-tail single aa mutations associated with ADPKD including a cluster of mutations in the G-protein binding and activation region of the PC1 C-tail that might affect G-protein signaling without affecting other properties of PC1. One such mutation is a three base pair deletion resulting in the deletion of a single conserved leucine residue (ΔL) within the PC1 C-tail (24).

In this study, we show that the ΔL mutation is one of several single aa mutations that significantly impairs G-protein signaling to AP-1 in transient transfection assays. Generation of a knock-in mutant mouse model ($Pkd1^{\Delta L}$) showed that this mutation causes a severe PKD phenotype. Homozygous $Pkd1^{\Delta L/\Delta L}$ mice are embryo lethal, similar to truncating loss-of-function mutations, and combination of $Pkd1^{\Delta L}$ with a conditional *Pkd1* deletion allele during embryonic development causes a severe cystic phenotype in pups. Although $Pkd1^{\Delta L}$ behaves like a null allele, normal levels of full-length $PC1^{\Delta L}$ protein product are made and produce GPS-cleaved and mature, glycosylated protein. The $PC1^{\Delta L}$ protein also forms complexes with PC2, yet is unable to support PC2 channel activity. As such, these experiments suggest that the G-protein binding and activation region of the C-tail is critical to PC1 function by regulating PC2 Ca^{2+} channel activity.

Results

PKD1 patient mutations within the G-protein binding region affect PC1 signaling

We had previously demonstrated that the C-terminal tail of PC1 binds and activates heterotrimeric G-proteins (16), and that PC1-mediated activation of JNK and AP-1 (12) is mediated by both Gα and Gβγ subunits (14). We also identified a polybasic G-protein activation domain (Fig. 1) that promotes nucleotide exchange, located within a highly conserved region of the PC1 C-tail required for stable binding of G-proteins (16). To determine whether mutations within this region affect PC1-mediated G-protein dependent signaling, we conducted a literature and database (pkdb.mayo.edu) (22) search to identify ADPKD patient mutations for further study. Our analysis identified a cluster of in-frame deletion or missense variants within

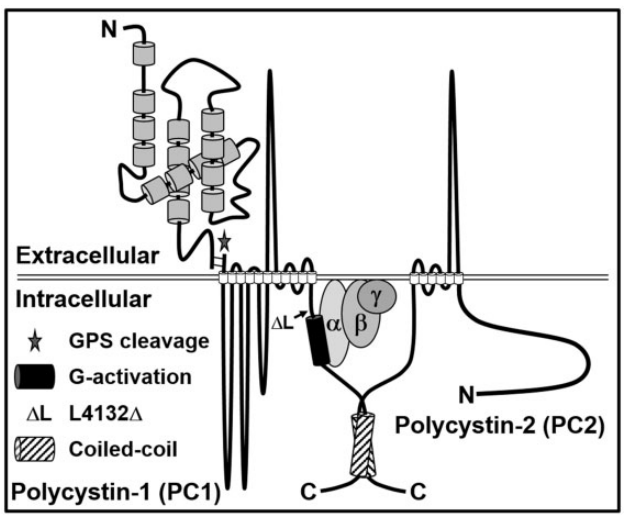

Figure 1. PC1 structure and C-tail sequence. The G-protein activation domain (G-activation, black cylinder) is a peptide region capable of activating nucleotide exchange of heterotrimeric G-proteins (αβγ). The site of ADPKD-associated human mutation L4132Δ (ΔL) is indicated by an arrow in the C-tail cytosolic domain. The coiled-coil (coiled-coil, hatched cylinder) mediates interactions with PC2. PC1 is cleaved at a G-protein coupled receptor proteolytic site (GPS cleavage, star) to produce N-and C-terminal fragments (NTF, CTF; respectively).

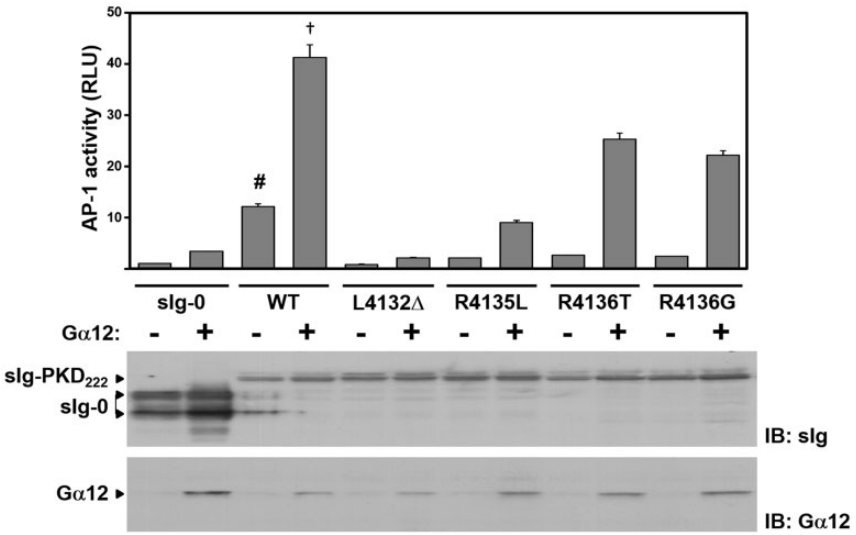

Figure 2. Effect of mutations in the G-protein activation region on AP-1 activation and G-protein augmented AP-1 activity. Expression of a WT C-terminal PC1 construct (sIg-PKD_{222}) activates an AP-1 promoter-reporter as compared to that in control- (sIg-0) transfected HEK293T cells. Single aa mutations L4132Δ, R4135L, R4136T and R4136G significantly reduce basal ($^{\#}P < 0.001$) and $G\alpha_{12}$-augmented ($^{\dagger}P < 0.001$) AP-1 activity compared to WT-expressing cells. Protein expression was confirmed by immunoblot (IB). $n = 3$. Data are means ± SE.

the G-protein binding domain in human PC1 (Supplementary Material, Fig. S1). To screen for function, corresponding mutations were introduced into a mouse PC1 C-tail fusion construct (sIg-PKD_{222}), and their effect on AP-1 activation was determined in transient transfection assays in HEK293T cells (14).

AP-1 activity was significantly stimulated by the WT sIg-PKD_{222} construct but was reduced in cells expressing sIg-PKD_{222} with patient mutations corresponding to L4132Δ, R4136T, R4136G (24–26) and engineered mutation R4135L (Fig. 2). An alanine substitution (L4132A) at the same site as L4132Δ did not have an effect on AP-1 activity (Supplementary Material, Fig. S2). These results show that mutations L4132Δ, R4135L, R4136T and R4136G interfere with AP-1 activation by the PC1 C-tail.

Previous work had shown that co-transfection of Gα subunits augmented AP-1 activation by WT sIg-PKD_{222} (14,15). To determine if the patient mutations would have an effect on Gα augmentation of AP-1 activation, HEK293T cells were co-transfected with $G\alpha_{12}$ or $G\alpha_q$ and WT or mutant sIg-PKD_{222} expression constructs. As previously observed, PC1-dependent AP-1 activity was augmented in cells co-expressing WT sIg-PKD_{222} and $G\alpha_{12}$ (Fig. 2). $G\alpha_{12}$-augmented activity was reduced in cells expressing R4136T or R4136G. Activity was further reduced in cells expressing the R4135L mutation, and was eliminated in cells expressing the L4132Δ mutant. Similar results were observed with co-expression of $G\alpha_q$ (Supplementary Material, Fig. S3A). Despite these pronounced effects on AP-1 activation, the mutant fusion proteins were able to interact and co-immunoprecipitate (IP) with co-transfected PC2 (Supplementary Material, Fig. S3B), consistent with these mutations not disrupting the coiled-coil region of PC1. These results suggest that the mutations specifically impair the ability of PC1 to activate heterotrimeric G-protein signaling. Of all the mutations studied, L4132Δ had the strongest effect on PC1-dependent AP-1 activation and was selected for further analysis.

Generation of $Pkd1^{NEO\,\Delta L}$ and $Pkd1^{\Delta L}$ mice

The human mutation L4132Δ (ΔL) was identified in an ADPKD family. The mutation was found in all affected family members, but not the unaffected parent, suggesting that L4132Δ was the causative mutation in that family (24). However, it could not be certain if this mutation was pathogenic, as the 5′ coding region of the *PKD1* gene was not examined for mutations in that analysis.

To determine whether the corresponding mouse ΔL mutation (L4122Δ) is sufficient to cause PKD, a targeting vector was constructed to introduce this mutation into mice using standard ES cell technology. Germline transmission of the $Pkd1^{NEO\,\Delta L}$ allele was observed in six founders, which were normal and viable. Proper integration of the targeting construct was verified by Southern blotting (Supplementary Material, Fig. S4).

To generate the $Pkd1^{\Delta L}$ allele, heterozygous $Pkd1^{NEO\,\Delta L/+}$ mice were crossed to a Cre-deleter strain (*EIIa-Cre*) to excise the floxed NEO cassette leaving a single, remnant *loxP* site within intron 45 (27). Excision was verified by genotyping using PCR primers that span the excised region and by sequence analysis (Supplementary Material, Fig. S4).

Characterization of $Pkd1^{NEO\,\Delta L}$ and $Pkd1^{\Delta L}$ transcripts

We reasoned that the presence of the floxed NEO cassette within intron 45 would interfere with proper splicing of the $Pkd1^{NEO\,\Delta L}$ transcript, effectively generating a null allele, and that *Cre*-mediated excision would restore splicing and proper transcription of $Pkd1^{\Delta L}$ message. To test this, RNA was isolated from mouse embryos and used as templates for RT-PCR using primers designed to selectively amplify $Pkd1^{+}$, $Pkd1^{NEO\,\Delta L}$ and $Pkd1^{\Delta L}$ transcripts. The results indicated that the $Pkd1^{NEO\,\Delta L}$ allele is most likely non-functional due to lack of intron 45 splicing. In contrast, the $Pkd1^{\Delta L}$ allele is properly spliced. As such, phenotypes arising from this allele are likely to be specific to the ΔL deletion (Supplementary Material, Fig. S5).

Characterization of $Pkd1^{NEO\,\Delta L}$ and $Pkd1^{\Delta L}$ mice

$Pkd1^{NEO\,\Delta L/+}$ mice were crossed with mice heterozygous for the $Pkd1^{m1Bei}$ allele, which is essentially null (28), to determine

whether the $Pkd1^{NEO\,\Delta L}$ allele behaves as a null. Of eight live births, zero animals were genotyped as $Pkd1^{NEO\,\Delta L/m1Bei}$. We next cultured E15.5 embryonic kidneys in the presence of 8-Br-cAMP. $Pkd1^{NEO\,\Delta L/m1Bei}$ kidneys developed cyst-like dilations (Supplementary Material, Fig. S6) as previously observed for $Pkd1^{m1Bei/m1Bei}$ kidneys (29). These dilations arise from CFTR- and NKCC1-mediated chloride-dependent fluid secretion, indicative of an underlying tubule disorder consistent with a lack of PC1 function. These results indicated that the $Pkd1^{NEO\,\Delta L}$ allele is non-functional.

To determine to what extent the $Pkd1^{\Delta L}$ mutation affects PC1 function, $Pkd1^{\Delta L/+}$ mice were crossed to generate $Pkd1^{\Delta L/\Delta L}$ mice. Of 100 live births, zero animals were genotyped as $Pkd1^{\Delta L/\Delta L}$, consistent with a severe, embryo lethal phenotype. E15.5 $Pkd1^{\Delta L/\Delta L}$ embryos were edematous (Fig. 3A). To verify the presence of cysts *in vivo*, embryonic kidneys were isolated at E15.5 and analyzed microscopically. Early cyst formation, including glomerular cysts, was observed in these kidney sections (Fig. 3B). Kidneys isolated from E15.5 pups and maintained in organ culture in the presence of 8-Br-cAMP developed large cyst-like dilations consistent with a loss of PC1 function (Fig. 3C).

To assess the effect of the ΔL allele on the growth and development of polycystic kidneys, and to circumvent the embryonic lethality, *Hoxb7-Cre:*$Pkd1^{\Delta L/cond}$ mice were generated (30,31). *Hoxb7-Cre:*$Pkd1^{\Delta L/cond}$ mice were born and had enlarged kidneys and elevated kidney weight to body weight ratios by P9 (Fig. 3D). Kidneys became even more enlarged by P14, with cyst formation throughout the entire kidney (Fig. 3E), comparable to cystic kidneys obtained from *Hoxb7-Cre:*$Pkd1^{cond/cond}$ mice (32). These results strongly suggest that the corresponding L4132Δ patient mutation is pathogenic.

Analysis of mutant PC1 protein

To determine how the ΔL deletion disrupts PC1 function, we asked whether the mutation affected PC1 expression or cleavage. Full-length WT, ΔL-mutated or coiled-coil truncating S4213X human PC1 proteins were expressed in HEK293T cells. Western blot analysis confirmed that the ΔL mutation did not affect PC1 protein expression levels, electrophoretic mobility or the ability of PC1 to undergo N- and C-terminal cleavage events (Fig. 4A). Full-length ΔL-mutated PC1 retained the ability to interact with PC2 in HEK293T cells in co-IP experiments (Fig. 4B), suggesting that the ΔL mutation does not disrupt the ability of PC1 to form complexes with PC2.

To determine whether the ΔL mutation affects cleavage or maturation of endogenous PC1 we examined membrane preparations from mouse embryonic fibroblasts (MEFs) isolated from E14.5 embryos. The preparations were treated with endoglycosidase H (EndoH; cleaves basic N-glycosides on immature proteins in the ER but is inactive toward glycosides on mature proteins processed in the Golgi) or peptide-N-glycosidase F (PNGaseF; cleaves oligosaccharides from both mature and immature proteins). Full-length protein, cleaved NTF and cleaved CTF were detected in $Pkd1^{\Delta L/\Delta L}$ MEF membrane preparations, and all glycoforms responded to EndoH and PNGaseF treatment in a manner identical to that of WT PC1 from $Pkd1^{+/+}$ MEF membranes (Fig. 5A and B). In a similar analysis, we observed that the product of the $Pkd1^{NEO\,\Delta L}$ allele was smaller than full-length PC1, and was cleaved to produce a single immature NTF glycoform that was entirely EndoH-sensitive (Fig. 5C). Given that the $Pkd1^{NEO\,\Delta L}$ mRNA fails to splice to exon 46 (Supplementary Material, Fig. S5B), the protein product most likely behaves like a C-terminal truncation

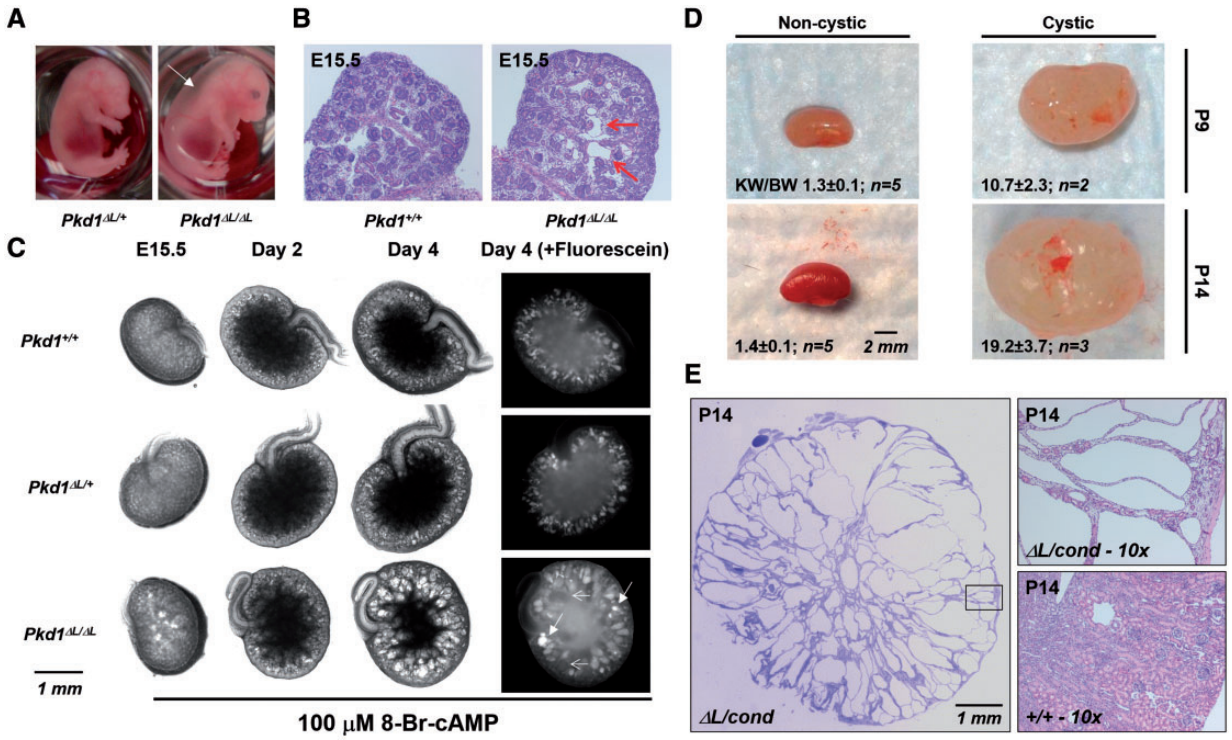

Figure 3. Analysis of $Pkd1^{L4122\Delta}$ (ΔL) kidneys. (**A**) E15.5 heterozygous embryos (ΔL/+; left) are normal. Homozygous embryos (ΔL/ΔL; right) are frequently inviable or exhibit edema (white arrow). (**B**) H&E-stained ΔL/ΔL kidneys revealed early cyst formation (arrows). (**C**) ΔL/ΔL kidneys developed severe cystic dilations following 4-day culturing in the presence of cAMP. Dilations of proximal tubular origin (broad arrows) as well as other nephron segments (narrow arrows) were detected by brief incubation with fluorescein, which is taken up by the proximal tubule. (**D**) *Hoxb7-Cre:*$Pkd1^{\Delta L/cond}$ pups exhibited massively enlarged kidneys at P9 and P14. E) H&E-stained kidneys from P14 *Hoxb7-Cre:*$Pkd1^{\Delta L/cond}$ pups revealed cyst formation throughout the entire kidney, as compared to a WT kidney (+/+).

mutant. These truncation mutants are known to undergo GPS cleavage but fail to mature beyond the ER due to an inability to interact with PC2, which is required for full maturation of PC1 (33,34). This is in marked contrast to the mature, full-length ΔL protein.

To determine whether the ΔL mutation affects PC1 protein levels, we quantified the amount of the PC1 glycoforms (full-length, mature and immature cleaved NTF) in membranes prepared from three independent WT and *Pkd1*$^{\Delta L/\Delta L}$ MEF cultures. The ΔL mutation did not affect the ratio of mature to immature NTF or the ratio of full-length PC1 relative to a membrane marker protein, ALIX, and there was only a small non-significant reduction in the amount of mature NTF relative to ALIX (Fig. 5C, and see discussion).

To determine whether the ΔL mutation affects PC1 intracellular membrane localization we analyzed protein from E14.5 whole embryo membrane preparations following fractionation over a heavy water/5–30% sucrose gradient (35) to separate membrane compartments. Immunoblot analysis of the total membrane preparations revealed comparable levels of full-length, and mature and immature NTF glycoforms of PC1 from WT and *Pkd1*$^{\Delta L/\Delta L}$ embryos (Fig. 6 and Supplementary Material, Fig. S7A). As observed with MEF cultures, mature NTF could not be detected in the total membrane preparation from *Pkd1*$^{NEO\,\Delta L/NEO\,\Delta L}$ embryos. Following centrifugation, gradient fractions were collected and analyzed by immunoblot. Full-length protein, mature NTF and immature NTF from both WT and PC1$^{\Delta L}$ protein had the same fractionation pattern across the entire spectrum of the gradient (Fig. 6 and Supplementary Material, Fig. S7A). In contrast, PC1$^{NEO\,\Delta L}$ protein had a qualitatively different fractionation pattern marked by decreased levels of mature NTF in peak fractions, increased levels of

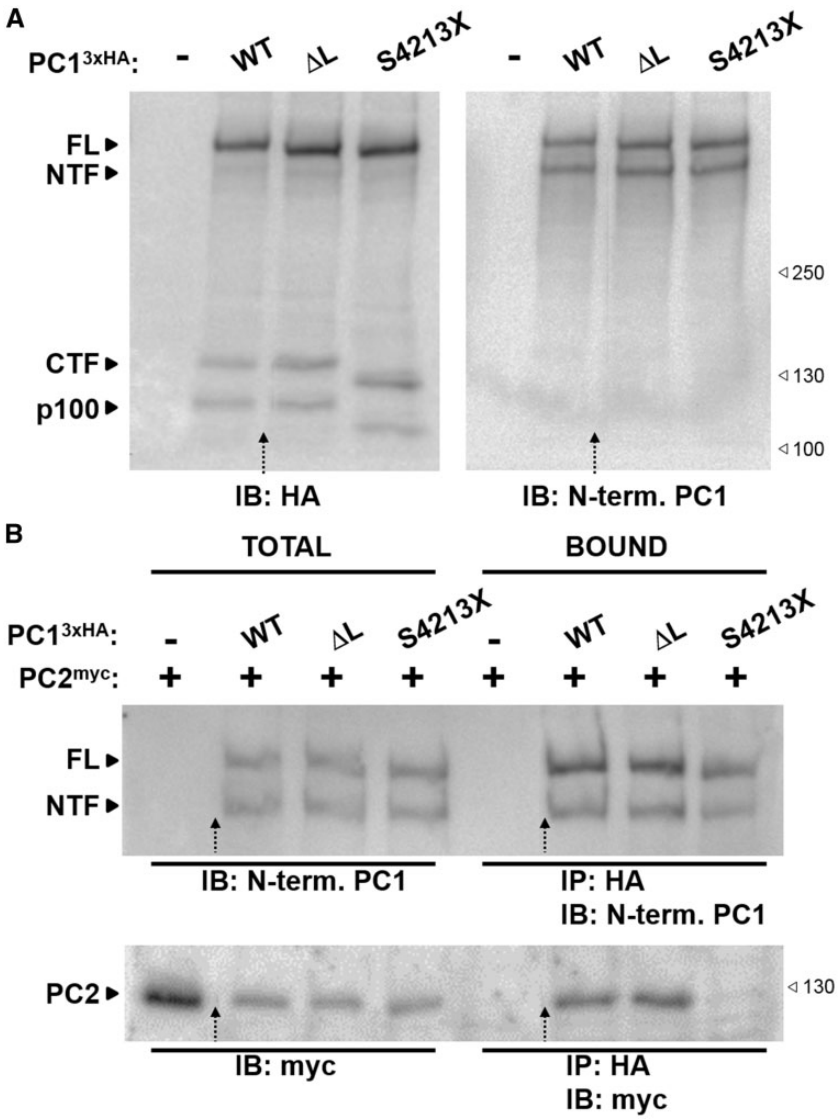

Figure 4. Expression of human PC1$^{\Delta L}$ and its interaction with PC2. (**A**) Full-length (FL) 3xHA-tagged (C-terminal) human PC1 proteins were expressed in HEK293T cells and detected with anti-HA (detects FL PC1, cleavage products CTF and p100, but not NTF) and N-terminal PC1 antibody 7E12 (detects FL and cleaved NTF, but not CTF and p100). PC1^{S4213X} is truncated just upstream of the coiled-coil domain (but also contains a C-terminal 3xHA tag), leading to faster migration of its CTF and p100 products. Dashed arrows indicate crop lines where separate portions of the same image are spliced together. (**B**) 3xHA-tagged PC1 and myc-tagged PC2 were expressed in HEK293T cells. Tagged PC1 was immunoprecipitated (IP'd) with anti-HA antibody and proteins were detected by IB with 7E12 for PC1 and anti-myc for PC2. The blot shows that PC1$^{\Delta L}$ is as capable as WT PC1 to interact with and IP PC2.

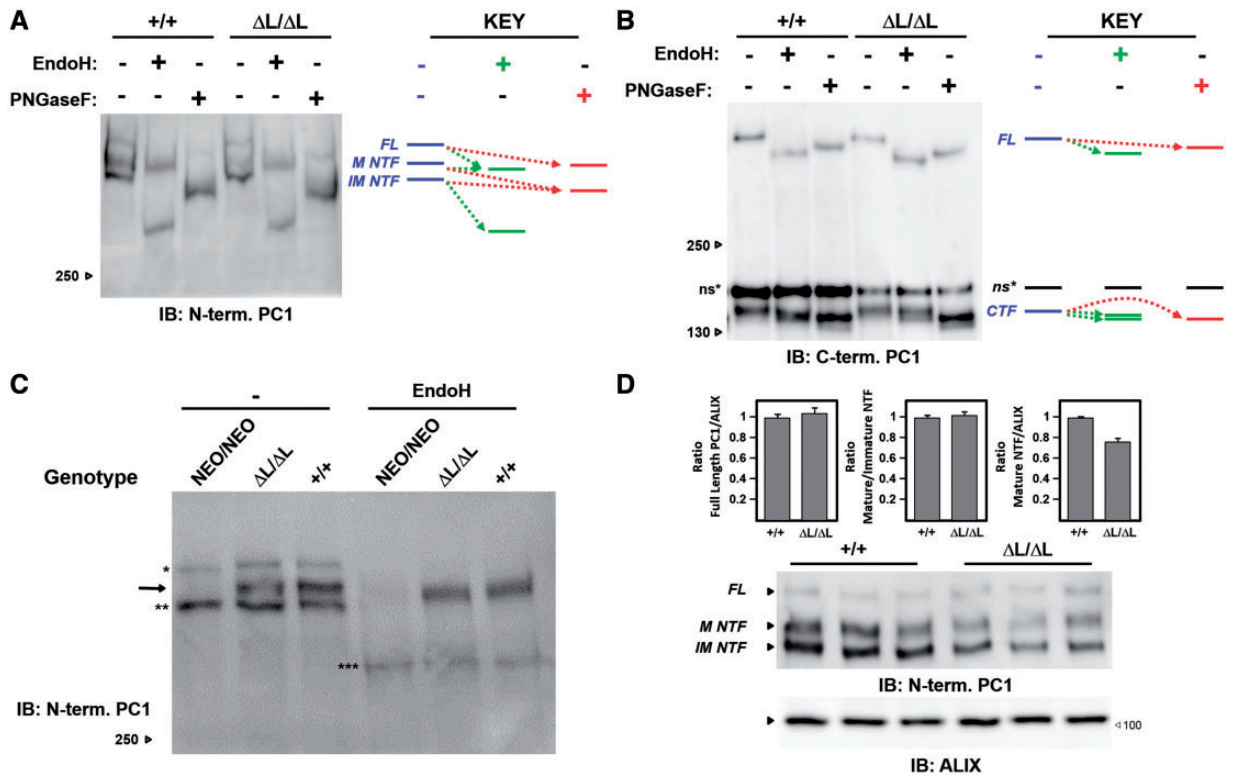

Figure 5. Expression and glycosylation of endogenous PC1$^{\Delta L}$ protein. (**A**) Mouse embryonic fibroblast (MEF) cultures were prepared from *Pkd1*ΔL/ΔL and *Pkd1*+/+ E14.5 embryos and treated with endoglycosidase H (EndoH) or peptide-N-glycosidase F (PNGaseF) to detect the maturation status of endogenous FL PC1 and GPS-cleaved NTF. PC1 was detected with 7E12. NTFs from *Pkd1*$^{+/+}$ and *Pkd1*$^{\Delta L/\Delta L}$ cells resolve into two distinct glycoforms (see key at right). The faster migrating band represents the immature (IM) glycoform of NTF which is sensitive to EndoH and the slower migrating band represents the mature (M) glycoform of NTF which is insensitive to EndoH. The uncleaved (FL) forms of PC1$^{\Delta L}$ and WT PC1 are also EndoH sensitive and their bands co-migrate with the mature NTF bands following digestion. The patterns for full-length and NTF glycoforms of PC1$^{\Delta L}$ and WT PC1 are identical. (**B**) Similar analysis was conducted to analyze maturation of the GPS-cleaved CTF using C-terminal PC1 antibody E8, which detects FL and CTF. Following EndoH, the CTF resolves into mature, EndoH-resistant (upper CTF band) and immature, EndoH-sensitive (lower CTF band) bands. Again, the digestion patterns for PC1ΔL and WT PC1 are identical. The E8 antibody detects a nonspecific band (*ns). (**C**) Membrane preparations from *Pkd1*$^{NEO\ \Delta L/NEO\ \Delta L}$ (NEO/NEO) were also analyzed with EndoH. Note the position of the full-length PC1$^{NEO\ \Delta L}$ protein (*) which is truncated due to the NEO insertion, and PC1$^{NEO\ \Delta L}$-derived, immature NTF before (**) and after (***) EndoH treatment. Also note the absence of mature NTF (arrow) in the untreated *Pkd1*$^{NEO\ \Delta L/NEO\ \Delta L}$ lane. (**D**) Endogenous PC1 levels were determined in MEF cultures isolated from three *Pkd1*$^{+/+}$ and three *Pkd1*$^{\Delta L/\Delta L}$ embryo littermates. The ΔL mutation did not affect the ratio of mature to immature NTF or the ratio of full-length PC1 relative to a membrane marker protein, ALIX, and there was only a small, non-significant (Student's *t*-test) reduction in the amount of mature NTF relative to ALIX.

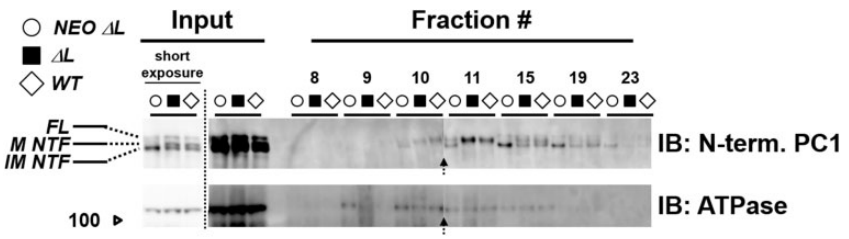

Figure 6. Cellular membrane fractionation of endogenous PC1$^{\Delta L}$ protein. Membrane preparations from *Pkd1*$^{NEO\Delta L/NEO\Delta L}$ (NEO ΔL, open circle), *Pkd1*$^{\Delta L/\Delta L}$ (ΔL, closed square) and *Pkd1*$^{+/+}$ (WT, open diamond) whole embryos were fractionated by centrifugation over heavy water/sucrose gradients. PC1 was detected in a total membrane aliquot (Input) and in gradient fractions by IB with 7E12. Localization of PC1 in plasma membrane fractions was confirmed by overlap with Na^+/K^+-ATPase (ATPase). The refractive index and complete gradient profile of PC1 from an independent experiment are shown in Supplementary Material, Figure S7A.

immature NTF, and the persistent presence of immature NTF toward the bottom of the gradient. These results suggest that the expression and membrane localization of PC1$^{\Delta L}$ is fundamentally identical to that of WT PC1. We also analyzed E14.5 embryonic kidneys for PC1 protein by immunoblotting. Full-length and mature NTF were easily detected in membrane preparations (Fig. 6 and Supplementary Material, Fig. S7A), but not in whole-cell kidney lysates where immature NTF was the only PC1 glycoform detected (Supplementary Material, Fig. S7B).

To confirm that PC1$^{\Delta L}$ protein was able to localize to the plasma membrane/cell surface, porcine LLC-PK1 cells were electroporated with constructs encoding GFP-tagged PC2 and either N-terminal mCherry-tagged WT PC1 or PC1$^{\Delta L}$ proteins (Fig. 7A) (33), and protein expression was confirmed in whole-cell lysates by immunoblot (Supplementary Material, Fig. S8A and B). PC1 was detected by immunofluorescence using antibody directed against the mCherry epitope tag under both non-permeabilized and permeabilized conditions (33). Under non-permeabilized

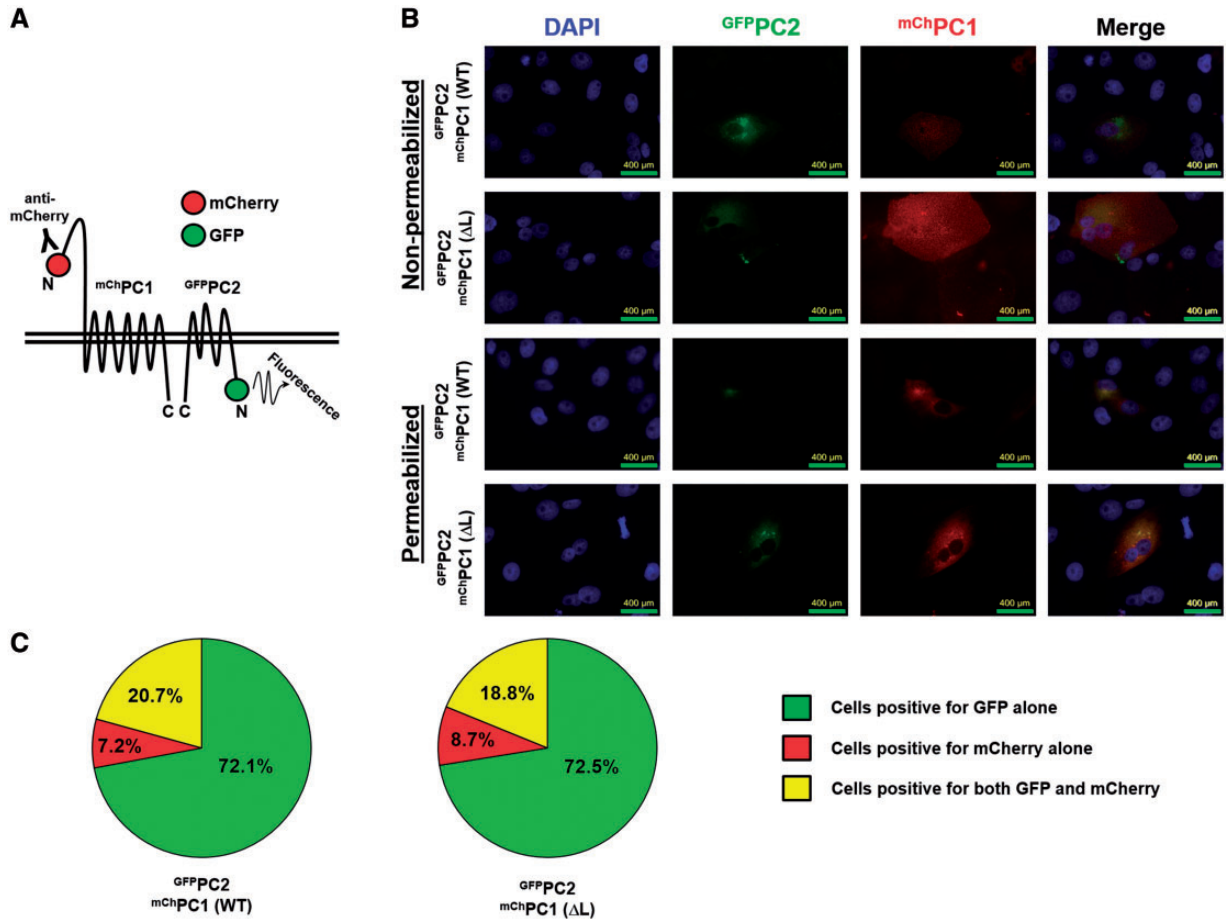

Figure 7. Surface expression of PC1$^{\Delta L}$ in porcine kidney epithelial cells. (**A**) LLC-PK1 cells were electroporated with constructs encoding ^{GFP}PC2 and ^{mCherry}PC1 (WT or ΔL), and analyzed by immunofluorescence. PC2 was detected using the intrinsic GFP fluorescence, and PC1 was detected using mCherry (mCh) antibodies. (**B**) Non-permeabilized conditions were used to detect surface PC1 expression, and permeabilized conditions were used to detect internal PC1 expression. (**C**) To determine the efficiency of PC1$^{\Delta L}$ trafficking to the cell surface (relative to WT PC1), GFP-positive cells in 5–10 random fields (non-permeabilized) were counted, followed by counting of mCherry-positive cells in the same fields. The percentage of all counted cells positive for GFP alone, mCherry alone or both GFP and mCherry is shown in the pie charts. Comparable transfection efficiency of the WT and ΔL constructs was confirmed by counting the number of cells positive for GFP, mCherry and GFP/mCherry signal as detected using permeabilized conditions (data not shown).

conditions, both WT and ΔL-mutated PC1 could be detected across the entire plasma membrane (Fig. 7B). Incubation without primary antibody to mCherry showed no PC1 detection (Supplementary Material, Fig. S8C). Under permeabilized conditions, both WT and ΔL-mutated PC1 were readily detected throughout the cell, with reduced immunofluorescence in the nuclear region (Fig. 7B). To determine whether PC1$^{\Delta L}$ trafficked as efficiently as WT PC1, we counted the number of cells that were positive for ^{GFP}PC2, ^{mCherry}PC1 or both in 5–10 fields from the non-permeabilized condition of three independent transfection experiments. For both WT PC1 and PC1$^{\Delta L}$, the majority of cells were positive for ^{GFP}PC2 only, and the percentage of cells positive for both ^{GFP}PC2 and ^{mCherry}PC1 was greater than for ^{mCherry}PC1 alone. Importantly, the total percentage of cells exhibiting surface expression of mCherry-PC1$^{\Delta L}$ (both with and without PC2) was essentially the same as for WT PC1 (Fig. 7C). These results confirm that the PC1$^{\Delta L}$ protein is capable of trafficking to the cell-surface in a manner comparable to that of WT PC1.

To determine if the ΔL mutation affects the ability of PC1 to regulate PC1/PC2 channel activity, we co-expressed human PC2 with either full-length WT PC1, PC1$^{\Delta L}$ or C-terminally truncated mutant PC1^{S4213X} in CHO cells and measured whole-cell macroscopic currents under voltage-clamp conditions (Fig. 8). Compared to cells expressing WT PC1, channel activity in cells expressing PC1$^{\Delta L}$ was reduced to levels comparable to that of cells expressing truncated PC1^{S4213X}, which cannot interact with PC2 (Figs 8A and 4B). To verify that the channel activity in CHO cells is PC2 dependent, we showed that a PC2 channel mutant, D511V (9), blocked activity to the same extent as both the PC1 truncation mutant and PC1$^{\Delta L}$ (Fig. 8B). Thus, it appears that the ΔL mutation inhibits PC1/PC2 channel activity without affecting the PC1/PC2 binding interaction.

Discussion

The majority of *PKD1* mutations analyzed has been shown to affect PC1 protein biogenesis, trafficking or stability and have revealed little about the intrinsic biochemical or cellular functions of PC1. In theory, analysis of missense *Pkd1* alleles has the potential to identify critical signaling domains and functional properties of PC1. We previously identified a highly conserved region within the C-terminal, cytosolic tail of PC1 that constitutes a minimal binding domain for heterotrimeric G-proteins

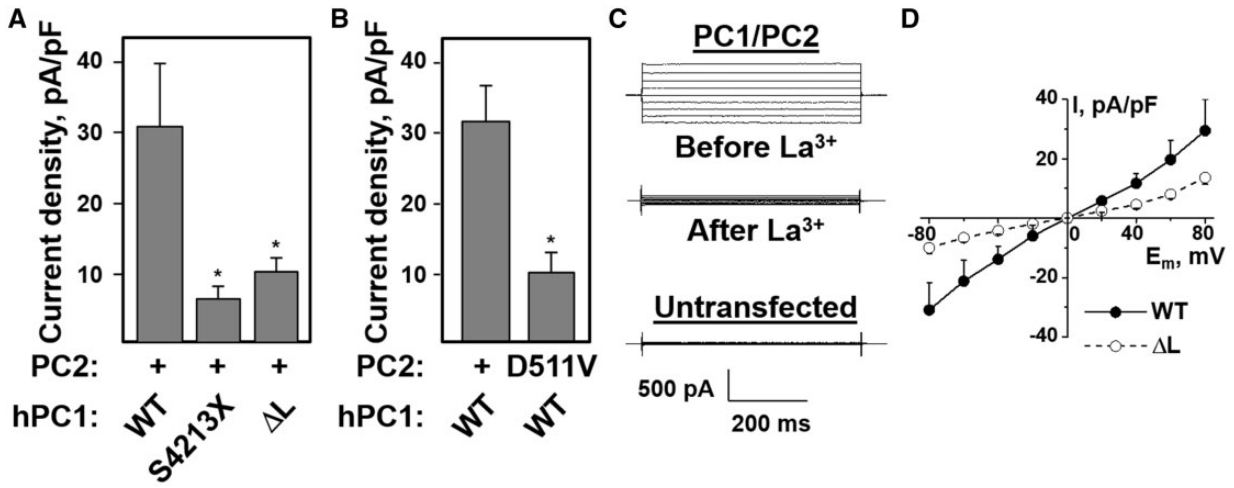

Figure 8. The PC1 ΔL mutation decreases PC1/PC2 channel activity. (**A**) La^{3+}-sensitive current density at −80 mV for voltage-clamped CHO cells expressing WT or mutant PC1 together with PC2 (*, $P < 0.05$, $n = 10$, 8 and 9, respectively from at least 4 independent transfections). (**B**) La^{3+}-sensitive current density at –80 mV for voltage-clamped CHO cells expressing WT or channel-defective (D511V) PC2 together with WT PC1 (*, $P < 0.05$, $n = 5$ and 7, respectively). (**C**) Representative current traces recorded from an individual cell overexpressing WT PC1/PC2 before and after superfusion with 0.5 mM La^{3+} and from an untransfected cell. (**D**) Current-voltage relationship in CHO cells expressing WT or ΔL mutant of PC1 and PC2 (E_m-voltage, I-density of La^{3+}-sensitive current).

and contains a 20 aa peptide sequence capable of activating heterotrimeric G-protein nucleotide exchange (16). To determine whether disruption of PC1-mediated activation of heterotrimeric G-protein signaling might be relevant to PKD, we analyzed ADPKD-associated missense mutations that lie in and around the G-protein activation domain using AP-1 activation as a surrogate for PC1-mediated heterotrimeric G-protein activity (14).

Human substitution mutations (R4135L, R4136T and R4136G) that removed the positive charge from the first two basic residues of the previously identified, polybasic G-protein activation peptide reduced PC1-mediated basal and Gα-augmented AP-1 activation without affecting the ability of PC1 to co-IP with PC2. Similar results were obtained for the single aa deletion L4132Δ (ΔL). Secondary structure algorithms (NPS@ and PORTER) (36,37) predict that L4132 lies within an amphipathic helix contiguous with and including the G-protein activation peptide. As such, deletion of L4132 would likely offset the distribution of multiple side-chain residues that could be important for PC1-mediated activation of heterotrimeric G-proteins (Supplementary Material, Fig. S9). An L4132A substitution at the same location, which we predicted would not alter the overall side-chain charge distribution, had no effect on PC1-mediated AP-1 activity.

We also noted the frequency of ADPKD-associated mutations affecting the G-protein activation domain (Supplementary Material, Fig. S10). While it may appear that there are no strong mutational hotspots when all loss-of-function mutations throughout the *PKD1* gene are considered (38), our analysis indicates that within the C-tail region there is a clustering of patient mutations within and around the conserved G-protein activation domain. Of the mutations studied here, human mutation L4132Δ (24) had the largest impact in an AP-1 transcriptional assay, blocking both basal and Gα-augmented activity. We selected this mutation for further analysis to determine pathogenicity and to gain insight into the importance and relevance of PC1-mediated G-protein signaling to PKD.

In all aspects tested, the $Pkd1^{\Delta L}$ allele behaves as a null allele. $Pkd1^{\Delta L/\Delta L}$ mice are embryo lethal, and *Hoxb7-Cre*:$Pkd1^{\Delta L/cond}$ mice develop severely cystic kidneys within the first 2 weeks following birth. A striking feature of the $Pkd1^{\Delta L}$ allele is that the $PC1^{\Delta L}$ protein shows normal expression, cleavage and maturation. In this regard, it is helpful to compare the properties of the $Pkd1^{\Delta L}$ allele to those of other missense *Pkd1* alleles such as $Pkd1^{RC}$, $Pkd1^{V}$ and $Pkd1^{m1Bei}$. Among these alleles, $Pkd1^{RC}$ has the least severe phenotype. $Pkd1^{RC/RC}$ mice have obvious renal defects by 3 months of age, but can survive up to a year of age (23). The $PC1^{RC}$ protein appears to be a temperature-sensitive folding mutant, with a ∼65% reduction in $PC1^{RC}$ protein levels relative to WT PC1 (33). $Pkd1^{V}$ is more severe, with $Pkd1^{V/V}$ mice exhibiting cystic defects by P4 and dying by about 1 month of age. Full-length $PC1^{V}$ is expressed, but fails to undergo GPS cleavage to produce NTF and CTF (39). $Pkd1^{m1Bei}$ is the most severe, with *in utero* cyst formation and embryonic lethality in $Pkd1^{m1Bei/m1Bei}$ animals (28). Analysis of the $PC1^{m1Bei1}$ protein revealed that it is expressed and undergoes GPS cleavage. However, the resulting cleavage products are sensitive to EndoH, indicating that it is unable to egress from the ER (34). As such, all three of these missense *Pkd1* alleles have PKD phenotypes because of decreased levels of mature, cleaved protein.

While the disease severity of the $Pkd1^{\Delta L}$ allele is comparable to that of $Pkd1^{m1Bei}$ and to *Pkd1* null alleles, our analysis of the $PC1^{\Delta L}$ protein reveals that there is at most only a small and non-significant decrease in the overall level of mature NTF. While this small reduction in mature NTF could in principle influence cystogenesis, it cannot account for the lethal phenotype. In a comparable experiment (33), MEFs isolated from $Pkd1^{+/-}$ embryos, which do not develop cystic disease, exhibit a greater reduction (∼50%) in mature NTF, establishing this as a threshold for sufficient PC1 function. MEFs isolated from $Pkd1^{RC/RC}$ embryos, which will develop only mild cystic disease as adults, exhibit a ∼65% reduction in mature NTF. In contrast, MEFs derived from severely cystic (embryo lethal) $Pkd1^{\Delta L/\Delta L}$ embryos have mature NTF levels that are well above these threshold levels, indicating that the embryonic lethality caused by the ΔL mutation cannot be explained by a reduction in $PC1^{\Delta L}$ expression relative to WT PC1.

Further evidence suggesting that $PC1^{\Delta L}$ protein expression and localization are comparable to those of WT PC1 was obtained by analyzing native protein in whole embryo

membrane preparations and in embryonic kidney lysates; and by analyzing proteins transiently expressed in porcine kidney epithelial cells. In all of these assays, the levels of $PC1^{\Delta L}$ expression, its fractionation profile, and its cellular localization were comparable to that of WT PC1. This was in marked contrast to the behavior of the protein produced from the $Pkd1^{\Delta L}$ precursor allele, $Pkd1^{NEO\,\Delta L}$, which does not produce appreciable levels of mature NTF, and has a different membrane fractionation profile. As such, our results indicate that the ΔL mutation disrupts a critical biochemical function of PC1.

In the current study, we sought to determine whether the ΔL mutation would affect the channel activity of PC2. Several lines of evidence suggest that PC2 channel activity might be affected by alterations in the ability of PC1 to activate heterotrimeric G-protein signaling (17,40). CHO cells expressing full-length PC1 and PC2 exhibited significantly higher channel activity than cells expressing PC2 and a C-terminally truncated $PC1^{S4213X}$ that cannot interact with PC2, or cells expressing PC1 and PC2 channel mutant, D511V (9), indicating that this channel activity requires the PC1/PC2 complex. Cells expressing full-length $PC1^{\Delta L}$ and PC2 had current levels comparable to that of channel-inactive $PC1^{S4213X}$/PC2 or $PC1/PC2^{D511V}$ cells. We believe that in these experiments the loss of PC2 channel activity occurs from an inability of the $PC1^{\Delta L}$ mutant to initiate G-protein signaling.

A disruption in PC1-mediated heterotrimeric G-protein signaling could potentially alter PC2 channel activity by several different mechanisms. For instance, PC2 localization and channel activity are regulated by phosphorylation (7,41–43), IP_3-induced Ca^{2+} release (44), and membrane lipid composition and intracellular Ca^{2+} (45–47). Each of these regulatory mechanisms involves second-messenger-dependent signaling that may be downstream of PC1-mediated G-protein signaling. PC2 could also be regulated through direct interactions with G-protein subunits activated by PC1. There are numerous examples of G-protein subunits directly regulating channel protein activity (48,49), a possibility that remains to be explored for PC2. Given these potential mechanisms, we speculate that the inability of the $PC1^{\Delta L}$ mutant to initiate G-protein signaling may result in an otherwise structurally normal PC1/PC2 complex that is functionally impaired.

Additional questions remain concerning the role of heterotrimeric G-protein signaling in PKD. Wu *et al.* demonstrated that in mice, *Pkd1* knockout leads to increased $G\alpha_{12}$ activation, and genetic deletion of *Gna12* blocks cystogenesis induced by deletion of *Pkd1*. In this model, PC1 is hypothesized to antagonize cystogenesis via its ability to sequester $G\alpha_{12}$ subunits in an inactive state (50). In a more recent study, Zhang *et al.* demonstrate a PKD phenotype in the *Xenopus* pronephric kidney following loss of the G-protein α subunit Gnas. However, this phenotype is antagonized by pharmacological and genetic inhibition of Gβγ signaling, suggesting that loss of Gnas leads to increased, cystogenic Gβγ signaling (51). Both of these results are in contrast with our model of PC1 signaling, which predicts that loss of PC1 signaling results in cystogenesis due to decreased heterotrimeric G-protein signaling. At this point it is difficult to reconcile these seemingly disparate models of PC1 function, but a common theme between Wu *et al.*, Zhang *et al.* and our present findings is the central importance of the PC1 G-protein binding domain to regulate heterotrimeric G-protein signaling (14,16).

In conclusion, our results have implications for treatment of PKD, as therapies designed to mimic or restore G-protein-mediated activation of PC2 may be sufficient to counteract cystogenesis in cases where PC1 is not expressed or incapable of activating G-proteins. Likewise, signaling mutants such as $PC1^{\Delta L}$ may be exquisitely responsive to small-molecule therapy designed to act specifically on inactive PC1/PC2 receptor-channel complexes. Future efforts should focus on revealing the molecular dynamics of the PC1/PC2 complex and the mechanisms by which PC1-activated G-protein subunits may regulate PC2 channel activity.

Materials and Methods

Detailed methods are available as supplementary material.

Plasmids

Plasmid sIg-PKD_{222} and sIg-0 were described previously (14). Mutations were introduced as previously described (52). 7xAP-1 Firefly luciferase reporter and pBlueScript were from Stratagene. Gα expression constructs were from the Missouri S&T cDNA Resource Center (www.cdna.org; date last accessed May 6, 2018). pRL-null was from Promega. PC2 expression plasmid pcDNA3 $PKD2^{myc}$ was provided by Leonidas Tsiokas (11); pTag ^{GFP}PC2 was described previously (33). The D511V mutation was introduced via PCR. Human PC1 expression plasmids were derived by subcloning *PKD1* sequences from AF20 and AF20 3xHA (provided by the Baltimore Polycystic Kidney Disease Research and Clinical Core Center) into pcDNA5/FRT/TO (Invitrogen) or ^{mCherry}PC1 (33). The *Pkd1* targeting vector was derived from a fragment containing mouse *Pkd1* exons 39–46 and a portion of the 3′ end of *Tsc2* isolated from a λ phage FIX II (Stratagene) library clone provided by Marianna Rodova (27). A floxed NEO cassette from pNTL (53) was inserted into intron 45, and the ΔL mutation was introduced with a QuikChangeII Site-Directed Mutagenesis Kit (Stratagene). All cloning manipulations were verified by DNA sequencing.

Cell culture, AP-1 assays, IP and Western blotting

HEK293T (ATCC) cells were transfected as described previously (14,15). AP-1 activity was determined with the dual luciferase assay kit (Promega) using an EG&G Berthold 9507 Luminometer. For co-IP following dual luciferase, sIg proteins were precipitated with EZ-View Protein A beads (Sigma) and proteins detected as described previously (14,52). For co-IP of full-length PC1 and PC2, HA-tagged PC1 was precipitated with agarose-conjugated HA-probe (F-7; Santa Cruz Biotech).

ES cell production

The targeting vector was linearized and electroporated into 129/Ola parental cells by the University of Kansas Medical Center Transgenic and Gene-Targeting Institutional Facility. Neomycin resistant clones were screened by long-range PCR. Positive clones were expanded and karyotyped, and proper recombination was verified by Southern blotting.

Southern blotting

ES cell or mouse tail DNA was isolated with the Wizard Genomic DNA Purification Kit (Promega), digested with BglII, and electrophoresed and detected by Southern blotting. Probe DNA was generated by PCR amplification of WT ES cell DNA. The product was cloned into pGEM-T (Promega), and an ~800 bp

NcoI fragment was labeled using the AlkPhos DIRECT kit (GE Healthcare).

Mice

Super-ovulated C57BL/6 females (The Jackson Laboratory) were mated to C57BL/6 males. Blastocysts were injected with *Pkd1*$^{NEO\,\Delta L}$ targeted ES cells and transferred to recipient CD-1 females (Charles River Laboratories). Chimeric mice were identified by agouti coloration and mated to C57BL/6 mice to obtain germline transmission. Agouti pups were genotyped by PCR and the presence of the *Pkd1*$^{NEO\,\Delta L}$ allele was verified by Southern. *Pkd1*$^{\Delta L}$ mice were generated by crossing F1 *Pkd1*$^{NEO\,\Delta L}$ heterozygotes to *EIIa-Cre* mice. The rearranged *Pkd1*$^{\Delta L}$ allele was detected by PCR and verified by DNA sequencing. *Hoxb7-Cre:Pkd1*$^{\Delta L/cond}$ mice were acquired by crossing *Pkd1*$^{\Delta L/+}$ and *Hoxb7-Cre:Pkd1*$^{cond/+}$ (30,31) mice. Phenotypic analysis was performed on mice of both sexes over a range of 2–4 backcrosses to C57BL/6. Total body weight and kidney weight were determined. Kidneys were fixed in formalin, paraffin embedded and stained with hematoxylin and eosin. All animal methods were approved by the University of Kansas Medical Center IACUC.

RNA isolation and RT-PCR

Kidney or brain tissue was homogenized in TRIzol (Invitrogen) and RNA was isolated per manufacturer's instructions. RNA was reverse transcribed with GoScript (Promega) and PCR was performed with GoTaq (Promega). Restriction digest with EcoRI (New England Biolabs) was used to distinguish WT from *Pkd1*$^{NEO\,\Delta L}$ or *Pkd1*$^{\Delta L}$ transcripts.

Organ culture

Metanephroi were dissected from embryonic mice and lysed in SDS-PAGE sample buffer or PC1 lysis buffer (Supplementary methods) for immunoblot analysis, or cultured ±100 μM 8-Br-cAMP and analyzed as described previously (29).

Mouse embryonic fibroblasts (MEFs)

Genotyped embryo carcasses were minced and digested twice with trypsin. Cells were maintained in DMEM (Cellgro) containing additional L-glutamine (2 mM) and 100 000 units penicillin/100 mg streptomycin per liter supplemented with 10% heat-inactivated fetal calf serum. Genotypes were verified after the first passage.

Deglycosylation assays

Total cellular membranes were purified from hyper-confluent MEF cultures as previously described (33) with minor modifications. Membrane fractions were treated with EndoH or PNGaseF (Promega) according to manufacturer's instructions with minor revisions.

Membrane preparation and sucrose gradient centrifugation

E14.5 embryos in lysis buffer were disrupted by polytron, Dounce homogenization and sonication. Membranes were clarified by gentle centrifugation, equilibrated and applied to a heavy water/5–30% sucrose gradient (35) and centrifuged at ~274 000*g* for 16 h in a Sorvall TH-641 rotor. Gradient fractions were collected from the top down using a BioComp fraction collector. The refractive index of each fraction was determined, and proteins were detected by immunoblotting.

Immunofluorescence

Porcine LLC-PK1 cells were electroporated (Nucleofector II; Amaxa with Basic Nucleofector Kit for Primary Mammalian Epithelial cells; Lonza) with pTAG ^{GFP}PC2 and ^{mCherry}PC1 constructs, and surface and intracellular expression of WT and ΔL-mutated PC1 was detected by immunofluorescence using antibody directed against the mCherry epitope (33). Images were obtained with an Eclipse TE2000-U microscope (Nikon) using a 60× oil objective and Image-Pro Premier (MediaCybernetics) and Photoshop (Adobe) software. For quantification, images were taken of 5–10 non-overlapping fields (20× objective) that contained GFP-positive cells. The same fields were subsequently imaged for Texas Red, and the number of cells positive for GFP, Texas Red or both was determined. Quantification was from three independent transfection experiments.

Electrophysiology

CHO cells (ATCC) were transfected using Polyfect reagent (Qiagen) as described previously (40,54) with green fluorescent protein (pEGFP-F; TaKaRa Clontech) and full-length PC1/PC2 expression constructs. Whole-cell macroscopic recordings of PC1/PC2 channel activity were made under voltage-clamp conditions on EGFP-positive cells 48–72 h after transfection as previously described (11,55) with an Axopatch 200B amplifier (Molecular Devices) interfaced via a Digidata 1440 (Molecular Devices) to a PC running the pClamp 10.3 software suite (Molecular Devices).

Secondary structure prediction analysis

Predictions were performed using NPS@ (Network Protein Sequence Analysis; https://npsa-prabi.ibcp.fr; date last accessed May 6, 2018) (36) and PORTER (37). Helical wheel projection analysis and hydrophobic moment calculations were performed at http://rzlab.ucr.edu/scripts/wheel/wheel.cgi; date last accessed May 6, 2018 (56).

Statistics

Data are means ± SE. Statistical significance was determined by one-way ANOVA and Student–Newman–Keuls (S–N–K) posttest for multiple comparisons.

Supplementary Material

Supplementary Material is available at *HMG* online.

Acknowledgements

The authors thank Marianna Rodova, Terry Peterson, Joshua Anderson and Lance Brandenburgh for generation of plasmids, Lynn Magenheimer for assistance maintaining mouse colonies, Darren Wallace for assistance with the manuscript, Don Armstrong for assistance with helical wheel predictions, Vladimir Gainullin for advice on PC1 deglycosylation assays, and the Baltimore Polycystic Kidney Disease Research and

Clinical Core Center, P30 DK090868, for plasmids and E8 antibody.

Conflict of Interest statement. None declared.

Funding

The study was supported by National Institutes of Health NS069759 (M.L.H.), 1F31NS076237 (M.A.H.), R35 HL135749 (A.S.), K99/R00 HL116603 (T.S.P.), P50 DK057301 (J.P.C.), P30 DK106912 (J.P.C.), American Heart Association 16EIA26720006 (A.S.) and a University of Kansas Medical Center Jared Grantham Kidney Institute Pilot and Feasibility award (S.C.P.). Funding to pay the Open Access publication charges for this article was provided by The Jared Grantham Kidney Institute PKD Rodent Model and Drug-Testing Core.

References

1. Cornec-Le Gall, E., Audrezet, M.P., Meur, Y.L., Chen, J.M. and Ferec, C. (2014) Genetics and pathogenesis of autosomal dominant polycystic kidney disease: 20 years on. *Hum. Mutat.*, **35**, 1393–1406.
2. Harris, P.C. and Torres, V.E. (2014) Genetic mechanisms and signaling pathways in autosomal dominant polycystic kidney disease. *J. Clin. Invest.*, **124**, 2315–2324.
3. Paul, B.M. and Vanden Heuvel, G.B. (2014) Kidney: polycystic kidney disease. *Wiley Interdiscip. Rev. Dev Biol*, **3**, 465–487.
4. Nims, N., Vassmer, D. and Maser, R.L. (2003) Transmembrane domain analysis of polycystin-1, the product of the polycystic kidney disease-1 (PKD1) gene: evidence for 11 membrane-spanning domains. *Biochemistry*, **42**, 13035–13048.
5. Promel, S., Langenhan, T. and Arac, D. (2013) Matching structure with function: the GAIN domain of adhesion-GPCR and PKD1-like proteins. *Trends Pharmacol. Sci.*, **34**, 470–478.
6. Hofherr, A. and Kottgen, M. (2011) TRPP channels and polycystins. *Adv. Exp. Med. Biol.*, **704**, 287–313.
7. Cai, Y., Anyatonwu, G., Okuhara, D., Lee, K.-B., Yu, Z., Onoe, T., Mei, C.-L., Qian, Q., Geng, L. and Wiztgall, R. (2004) Calcium dependence of polycystin-2 channel activity is modulated by phosphorylation at Ser812. *J. Biol. Chem.*, **279**, 19987–19995.
8. Ćelić, A.S., Petri, E.T., Benbow, J., Hodsdon, M.E., Ehrlich, B.E. and Boggon, T.J. (2012) Calcium-induced conformational changes in C-terminal tail of polycystin-2 are necessary for channel gating. *J. Biol. Chem.*, **287**, 17232–17240.
9. Koulen, P., Cai, Y., Geng, L., Maeda, Y., Nishimura, S., Witzgall, R., Ehrlich, B.E. and Somlo, S. (2002) Polycystin-2 is an intracellular calcium release channel. *Nat. Cell Biol.*, **4**, 191–197.
10. Qian, F., Germino, F.J., Cai, Y., Zhang, X., Somlo, S. and Germino, G.G. (1997) PKD1 interacts with PKD2 through a probable coiled-coil domain. *Nat. Genet.*, **16**, 179–183.
11. Hanaoka, K., Qian, F., Boletta, A., Bhunia, A.K., Piontek, K., Tsiokas, L., Sukhatme, V.P., Guggino, W.B. and Germino, G.G. (2000) Co-assembly of polycystin-1 and -2 produces unique cation-permeable currents. *Nature*, **408**, 990–994.
12. Arnould, T., Kim, E., Tsiokas, L., Jochimsen, F., Grüning, W., Chang, J.D. and Walz, G. (1998) The polycystic kidney disease 1 gene product mediates protein kinase C alpha-dependent and c-Jun N-terminal kinase-dependent activation of the transcription factor AP-1. *J. Biol. Chem.*, **273**, 6013–6018.
13. Le, N.H., van der Bent, P., Huls, G., van de Wetering, M., Loghman-Adham, M., Ong, A.C.M., Calvet, J.P., Clevers, H., Breuning, M.H., van Dam, H. *et al.* (2004) Aberrant polycystin-1 expression results in modification of activator protein-1 activity, whereas Wnt signaling remains unaffected. *J. Biol. Chem.*, **279**, 27472–27481.
14. Parnell, S.C., Magenheimer, B.S., Maser, R.L., Zien, C.A., Frischauf, A.-M. and Calvet, J.P. (2002) Polycystin-1 activation of c-Jun N-terminal kinase and AP-1 is mediated by heterotrimeric G proteins. *J. Biol. Chem.*, **277**, 19566–19572.
15. Puri, S., Magenheimer, B.S., Maser, R.L., Ryan, E.M., Zien, C.A., Walker, D.D., Wallace, D.P., Hempson, S.J. and Calvet, J.P. (2004) Polycystin-1 activates the calcineurin/NFAT (nuclear factor of activated T-cells) signaling pathway. *J. Biol. Chem.*, **279**, 55455–55464.
16. Parnell, S.C., Magenheimer, B.S., Maser, R.L., Rankin, C.A., Smine, A., Okamoto, T. and Calvet, J.P. (1998) The polycystic kidney disease-1 protein, polycystin-1, binds and activates heterotrimeric G-proteins in vitro. *Biochem. Biophys. Res. Commun.*, **251**, 625–631.
17. Delmas, P., Nomura, H., Li, X., Lakkis, M., Luo, Y., Segal, Y., Fernández-Fernández, J.M., Harris, P., Frischauf, A.-M., Brown, D.A. *et al.* (2002) Constitutive activation of G-proteins by polycystin-1 is antagonized by polycystin-2. *J. Biol. Chem.*, **277**, 11276–11283.
18. Nauli, S.M., Alenghat, F.J., Luo, Y., Williams, E., Vassilev, P., Li, X., Elia, A.E.H., Lu, W., Brown, E.M., Quinn, S.J. *et al.* (2003) Polycystins 1 and 2 mediate mechanosensation in the primary cilium of kidney cells. *Nat. Genet.*, **33**, 129–137.
19. DeCaen, P.G., Delling, M., Vien, T.N. and Clapham, D.E. (2013) Direct recording and molecular identification of the calcium channel of primary cilia. *Nature*, **504**, 315–318.
20. Delling, M., DeCaen, P.G., Doerner, J.F., Febvay, S. and Clapham, D.E. (2013) Primary cilia are specialized calcium signalling organelles. *Nature*, **504**, 311–314.
21. Jin, X., Mohieldin, A.M., Muntean, B.S., Green, J.A., Shah, J.V., Mykytyn, K. and Nauli, S.M. (2014) Cilioplasm is a cellular compartment for calcium signaling in response to mechanical and chemical stimuli. *Cell. Mol. Life Sci.* **71**, 2165–2178.
22. Autosomal Dominant Polycystic Kidney Disease: Mutation Database. http://pkdb.mayo.edu: Updated 2014; date last accessed May 6, 2018.
23. Hopp, K., Ward, C.J., Hommerding, C.J., Nasr, S.H., Tuan, H.-F., Gainullin, V.G., Rossetti, S., Torres, V.E. and Harris, P.C. (2012) Functional polycystin-1 dosage governs autosomal dominant polycystic kidney disease severity. *J. Clin. Invest.*, **122**, 4257–4273.
24. Afzal, A.R., Hand, M., Ternes-Pereira, E., Saggar-Malik, A., Taylor, R. and Jeffery, S. (1999) Novel mutations in the 3 region of the polycystic kidney disease 1 (PKD1) gene. *Hum. Genet.*, **105**, 648–653.
25. Gagnon, J.-S., Hupe, P., Arthus, M.-F., Lonergan, M., Nawar, T., Morgan, K., Fujiwara, T.M. and Bichet, D.G. (1998) PKD1 mutation and polymorphisms in French-Canadian families. *J. Am. Soc. Nephrol.*, **9**, 373A.
26. Perrichot, R.A., Mercier, B., Simon, P.M., Whebe, B., Cledes, J. and Ferec, C. (1999) DGGE screening of PKD1 gene reveals novel mutations in a large cohort of 146 unrelated patients. *Hum. Genet.*, **105**, 231–239.
27. Rodova, M., Islam, M.R., Peterson, K.R. and Calvet, J.P. (2003) Remarkable sequence conservation of the last intron in the PKD1 gene. *Mol. Biol. Evol.*, **20**, 1669–1674.
28. Herron, B.J., Lu, W., Rao, C., Liu, S., Peters, H., Bronson, R.T., Justice, M.J., McDonald, J.D. and Beier, D.R. (2002) Efficient

generation and mapping of recessive developmental mutations using ENU mutagenesis. *Nat. Genet.*, **30**, 185–189.
29. Magenheimer, B.S., St John, P.L., Isom, K.S., Abrahamson, D.R., De Lisle, R.C., Wallace, D.P., Maser, R.L., Grantham, J.J. and Calvet, J.P. (2006) Early embryonic renal tubules of wild-type and polycystic kidney disease kidneys respond to cAMP stimulation with cystic fibrosis transmembrane conductance regulator/Na(+), K(+), 2Cl(-) Co-transporter-dependent cystic dilation. *J. Am. Soc. Nephrol.*, **17**, 3424–3437.
30. Piontek, K.B., Huso, D.L., Grinberg, A., Liu, L., Bedja, D., Zhao, H., Gabrielson, K., Qian, F., Mei, C., Westphal, H. *et al.* (2004) A functional floxed allele of Pkd1 that can be conditionally inactivated in vivo. *J. Am. Soc. Nephrol.*, **15**, 3035–3043.
31. Yu, J., Carroll, T.J. and McMahon, A.P. (2002) Sonic hedgehog regulates proliferation and differentiation of mesenchymal cells in the mouse metanephric kidney. *Development*, **129**, 5301–5312.
32. Paul, B.M., Vassmer, D., Taylor, A., Magenheimer, L., Carlton, C.G., Piontek, K.B., Germino, G.G. and Vanden Heuvel, G.B. (2011) Ectopic expression of Cux1 is associated with reduced p27 expression and increased apoptosis during late stage cyst progression upon inactivation of Pkd1 in collecting ducts. *Dev. Dyn.*, **240**, 1493–1501.
33. Gainullin, V.G., Hopp, K., Ward, C.J., Hommerding, C.J. and Harris, P.C. (2015) Polycystin-1 maturation requires polycystin-2 in a dose-dependent manner. *J. Clin. Invest.*, **125**, 607–620.
34. Kurbegovic, A., Kim, H., Xu, H., Yu, S., Cruanès, J., Maser, R.L., Boletta, A., Trudel, M. and Qian, F. (2014) Novel functional complexity of polycystin-1 by GPS cleavage in vivo: role in polycystic kidney disease. *Mol. Cell. Biol.*, **34**, 3341–3353.
35. Hogan, M.C., Bakeberg, J.L., Gainullin, V.G., Irazabel, M.V., Harmon, A.J., Lieske, J.C., Charlesworth, M.C., Johnson, K.L., Madden, B.J., Zenka, R.M. *et al.* (2014) Identification of biomarkers for PKD1 using urinary exosomes. *J. Am. Soc. Nephrol.*, **26**: 1661–70.
36. Combet, C., Blanchet, C., Geourjon, C. and Deleage, G. (2000) NPS@: network protein sequence analysis. *Trends Biochem. Sci.*, **25**, 147–150.
37. Pollastri, G. and McLysaght, A. (2005) Porter: a new, accurate server for protein secondary structure prediction. *Bioinformatics*, **21**, 1719–1720.
38. Rossetti, S., Strmecki, L., Gamble, V., Burton, S., Sneddon, V., Peral, B., Roy, S., Bakkaloglu, A., Komel, R., Winearls, C.G. *et al.* (2001) Mutation analysis of the entire PKD1 gene: genetic and diagnostic implications. *Am. J. Hum. Genet.*, **68**, 46–63.
39. Yu, S., Hackmann, K., Gao, J., Gao, J., He, X., Piontek, K., García-González, M.A., García González, M.A., Menezes, L.F., Xu, H. *et al.* (2007) Essential role of cleavage of Polycystin-1 at G protein-coupled receptor proteolytic site for kidney tubular structure. *Proc. Natl. Acad. Sci. U. S. A.*, **104**, 18688–18693.
40. Kwon, M., Pavlov, T.S., Nozu, K., Rasmussen, S.A., Ilatovskaya, D.V., Lerch-Gaggl, A., North, L.M., Kim, H., Qian, F., Sweeney, W.E. *et al.* (2012) G-protein signaling modulator 1 deficiency accelerates cystic disease in an orthologous mouse model of autosomal dominant polycystic kidney disease. *Proc. Natl. Acad. Sci. U. S. A.*, **109**, 21462–21467.
41. Cantero, M. d R., Velázquez, I.F., Streets, A.J., Ong, A.C.M. and Cantiello, H.F. (2015) The cAMP signaling pathway and direct protein kinase a phosphorylation regulate polycystin-2 (TRPP2) channel function. *J. Biol. Chem.*, **290**, 23888–23896.
42. Streets, A.J., Needham, A.J., Gill, S.K. and Ong, A.C. (2010) Protein kinase D-mediated phosphorylation of polycystin-2 (TRPP2) is essential for its effects on cell growth and calcium channel activity. *Mol. Biol. Cell*, **21**, 3853–3865.
43. Streets, A.J., Wessely, O., Peters, D.J. and Ong, A.C. (2013) Hyperphosphorylation of polycystin-2 at a critical residue in disease reveals an essential role for polycystin-1-regulated dephosphorylation. *Hum. Mol. Genet.*, **22**, 1924–1939.
44. Sammels, E., Devogelaere, B., Mekahli, D., Bultynck, G., Missiaen, L., Parys, J.B., Cai, Y., Somlo, S. and De Smedt, H. (2010) Polycystin-2 activation by inositol 1, 4, 5-trisphosphate-induced Ca2+ release requires its direct association with the inositol 1, 4, 5-trisphosphate receptor in a signaling microdomain. *J. Biol. Chem.*, **285**, 18794–18805.
45. Grieben, M., Pike, A.C.W., Shintre, C.A., Venturi, E., El-Ajouz, S., Tessitore, A., Shrestha, L., Mukhopadhyay, S., Mahajan, P., Chalk, R. *et al.* (2017) Structure of the polycystic kidney disease TRP channel Polycystin-2 (PC2). *Nat. Struct. Mol. Biol.*, **24**, 114–122.
46. Shen, P.S., Yang, X., DeCaen, P.G., Liu, X., Bulkley, D., Clapham, D.E. and Cao, E. (2016) The structure of the polycystic kidney disease channel PKD2 in lipid nanodiscs. *Cell*, **167**, 763–773.
47. Wilkes, M., Madej, M.G., Kreuter, L., Rhinow, D., Heinz, V., De Sanctis, S., Ruppel, S., Richter, R.M., Joos, F., Grieben, M. *et al.* (2017) Molecular insights into lipid-assisted Ca(2+) regulation of the TRP channel Polycystin-2. *Nat. Struct. Mol. Biol.*, **24**, 123–130.
48. Wettschureck, N. and Offermanns, S. (2005) Mammalian G proteins and their cell type specific functions. *Physiol. Rev.*, **85**, 1159–1204.
49. Zhang, X., Mak, S., Li, L., Parra, A., Denlinger, B., Belmonte, C. and McNaughton, P.A. (2012) Direct inhibition of the cold-activated TRPM8 ion channel by Galphaq. *Nat. Cell Biol.*, **14**, 851–858.
50. Wu, Y., Xu, J.X., El-Jouni, W., Lu, T., Li, S., Wang, Q., Tran, M., Yu, W., Wu, M., Barrera, I.E. *et al.* (2016) Galpha12 is required for renal cystogenesis induced by Pkd1 inactivation. *J. Cell Sci.*, **129**, 3675–3684.
51. Zhang, B., Tran, U. and Wessely, O. (2018) Polycystin 1 loss of function is directly linked to an imbalance in G-protein signaling in the kidney. *Development*, **145**, . pii: dev158931.
52. Parnell, S.C., Puri, S., Wallace, D.P. and Calvet, J.P. (2012) Protein phosphatase-1alpha interacts with and dephosphorylates polycystin-1. *PLoS One*, **7**, e36798.
53. Abuin, A. and Bradley, A. (1996) Recycling selectable markers in mouse embryonic stem cells. *Mol. Cell. Biol.*, **16**, 1851–1856.
54. Staruschenko, A., Booth, R.E., Pochynyuk, O., Stockand, J.D. and Tong, Q. (2006) Functional reconstitution of the human epithelial Na+ channel in a mammalian expression system. *Methods Mol. Biol.*, **337**, 3–13.
55. Babich, V., Zeng, W.-Z., Yeh, B.-I., Ibraghimov-Beskrovnaya, O., Cai, Y., Somlo, S. and Huang, C.-L. (2004) The N-terminal extracellular domain is required for polycystin-1-dependent channel activity. *J. Biol. Chem.*, **279**, 25582–25589.
56. Zidovetzki, R., Rost, B., Armstrong, D.L. and Pecht, I. (2003) Transmembrane domains in the functions of Fc receptors. *Biophys. Chem.*, **100**, 555–575.